HHS Public Access

Author manuscript

Mol Genet Metab. Author manuscript; available in PMC 2020 October 07.

Published in final edited form as:

Mol Genet Metab. 2017 August ; 121(4): 314–319. doi:10.1016/j.ymgme.2017.06.009.

Analyses of *SLC13A5*-epilepsy patients reveal perturbations of TCA cycle

Matthew N Bainbridge, Ph.D.[1,2,3], **Erin Cooney, M.D.**[4], **Marcus Miller, Ph.D.**[4], **Adam Kennedy, Ph.D.**[5], **Jacob Wulff, Ph.D.**[5], **Taraka Donti, Ph.D.**[4], **Shalini N Jhangiani, M.S.**[1], **Richard A Gibbs, Ph.D.**[1], **Sarah H. Elsea, Ph.D.**[4], **Brenda E. Porter, M.D.**[6], **Brett H. Graham, M.D., Ph.D.**[4]

[1]Human Genome Sequencing Center, Baylor College of Medicine, Houston, TX

[2]Codified Genomics LLC, Houston, TX

[3]Institute for Genomic Medicine, Rady Children's Hospital, San Diego, CA

[4]Dept. of Molecular and Human Genetics, Baylor College of Medicine, Houston, TX

[5]Metabolon, Morrisville, NC

[6]Department of Neurology, Stanford University Medical School, Palo Alto, CA

Abstract

Objective—To interrogate the metabolic profile of five subjects from three families with rare, nonsense and missense mutations in *SLC13A5* and Early Infantile Epileptic Encephalopathies (EIEE) characterized by severe, neonatal onset seizures, psychomotor retardation and global developmental delay.

Methods—Mass spectrometry of plasma, CSF and urine was used to identify consistently dysregulated analytes in our subjects.

Results—distinctive elevations of citrate and dysregulation of citric acid cycle intermediates, supporting the hypothesis that loss of SLC13A5 function alters tricarboxylic acid cycle (TCA) metabolism and may disrupt metabolic compartmentation in the brain.

Significance—Our results indicate that analysis of plasma citrate and other TCA analytes in *SLC13A5* deficient patients define a diagnostic metabolic signature that can aid in diagnosing children with this disease.

Keywords

SLC13A5; tricarboxylic acid cycle; seizure; metabolomics

Corresponding author: Brett Graham, 1 Baylor Plaza, Houston, TX, 77030, 713-798-6209, 713-798-7773, bgraham@bcm.edu.

Conflicts of Interest

MNB is a founder of Codified Genomics LLC a variant interpretation company. The other authors declare no conflicts of interest.

INTRODUCTION

Epilepsy can be a devastating disease and can be caused by both environmental and genetic factors and can often lead to developmental delay[1]. Early Infantile Epileptic Encephalopathies (EIEE) are a heterogeneous group of disorders characterized by refractory seizures with onset in the first year of life, often associated with cognitive, sensory and motor abnormalities comorbid with clinical and subclinical epileptic activity [2]. Etiologies of EIEE include structural brain malformations, inborn errors of metabolism, and injury as well as genetic causes. Monogenic causes have been well described and include disturbances in neuronal ion channels (e.g. *SCN1A* [3] and *KCNQ2*), neurotransmitter receptors (e.g. *GABRB3* [4] and *CHRNA2*), and mitochondrial function (e.g. RARS2 [5]). The genetic heterogeneity of monogenic forms is also manifested by multiple examples of autosomal dominant (both *de novo* and inherited with variable penetrance), autosomal recessive, and X-linked forms [6].

Recent publications have identified compound heterozygous and homozygous mutations in *SLC13A5* as an autosomal recessive, monogenic etiology of EIEE25 [MIM: 608305] [7,8] and one of two genes that cause Kohlschütter-Tönz syndrome [MIM: 614574][9]. SLC13A5 is an inward-directed electrogenic sodium-coupled tricarboxylate substrate transporter predominantly expressed in liver and diffuse expression throughout the brain. *SLC13*A5 is located at 17p13.1, consists of 11 exons and has both eukaryotic and prokaryotic homologs [10]. The tricarboxylate transporter contains 12 transmembrane domains and exhibits highest affinity for citrate with significantly lower affinity for other tricarboxylic acid (TCA) cycle intermediates such as succinate, fumarate and malate [11]. *SLC13A5* is the homolog of the fruit fly *INDY* gene [12], which had previously been associated with longevity, although this association is disputed [13]. Mouse knockouts of *Slc13a5* are smaller in size, show insulin resistance and protection against obesity [14]. Hepatic content of ATP is sharply reduced and mitochondrion metabolism and mitochondrion-associated gene-expression are increased. The mechanism of action in both fruit fly and mouse is thought to be due to mimicking calorie restriction and in *C. elegans SLC13A5* (Indy/CeNac2) knockdowns have been shown to induce *AMPK* [15]. Interestingly, no neurological phenotype was reported for either fruit fly or mice [13,14]. Although mutations in *SLC13A5* are strongly associated with EIEE25, the underlying causal mechanism is unknown. There are two reports in the literature using heterologous expression systems to suggest that cases of SLC13A5 deficiency are associated with loss of citrate transport activity [8,16].

Understanding the potential effects of primary or secondary perturbations of energy metabolism is crucial in understanding and controlling seizures [17]. The tricarboxylic acid cycle (TCA) is critical for brain function, not only for energy production but as a supply of biosynthetic precursors for amino acids and neurotransmitters [18]. Citrate is a major substrate for energy generation in most cells, is detectable in plasma, and is taken up into cells by the SCL13 family of transporters [19]. Based on recent transcriptomic studies, *SLC13A5* is expressed at high levels in adult astrocytes, with lower expression in other brain cell types, including neurons [20,21]. Neurons lack the capacity to perform *de novo* synthesis of tricarboxylic acid (TCA) cycle constituents (anaplerosis) owing to the absence of pyruvate carboxylase, and are dependent on astrocytes to supply lactate, glutamine, alpha-

ketoglutarate (aKG) and other metabolites [22]. Here, we utilize mass spectrometric methods to analyze the CSF, plasma, and urine metabolites of five patients from three families to determine the metabolic derangements due to *SLC13A5* loss of function.

SUBJECTS/MATERIALS AND METHODS

This research was conducted under IRB approval from Baylor College of Medicine and Stanford University with informed consent from the parents of the affected subjects. All work was done in accordance of the Helsinki Declaration of 1975, as revised in 2000.

Metabolomic analysis was performed as described previously [23]. Median raw intensity values were calculated for all analytes identified in >=2/3 of the anchor specimen and these median values were then used to normalize corresponding analyte raw intensity values in patient specimen. Analytes not identified in 2/3 or more of the anchor specimens were excluded from analysis. Anchor adjusted analyte values are individually median scaled to control samples and log transformed. For urine specimen, raw intensity values were normalized to osmolality and creatinine prior to anchoring. P-values for analytes were calculated using the heteroscedastic Student's T-test. FDR was calculated using the technique of Benjamini and Hochberg.

Sequence data was generated on the Illumina HiSeq 2000 platform Reads were aligned, variants called, annotated and prioritized as previously described [24].

Patient Description

Subjects A1 and A2 (previously described [16]) are the 1st and 4th children born to healthy, non-consanguineous parents of western European ancestry (Figure 1A). Subject A1 was noted to have seizure activity within the first 24 hours of life. Her seizures have been refractory despite dozens of antiepileptic drug regimens, including cannabinoid trial and vagal nerve stimulator. Shortly after starting a ketogenic diet Subject A1 went into status epilepticus necessitating a medically induced coma. Brain MRIs have all been unremarkable. Subject A1 has short stature (FOC 57 cm, z=2.20; weight 41.5 kg, z=−0.5; length 141.3 cm, z=−2.22). Subject A2 is a nondysmorphic, 3-year-old male born full term after an uncomplicated pregnancy with seizures starting within the first 24 hours of life. His current seizure burden is approximately 5–8 seizures per year. Subject A2 had failure to thrive in the first 2 years of life, but by age 3-years has normal growth parameters (FOC 49.1 cm, z=−0.71, weight 14.1 kg, z=−0.51, length 94.8 cm, z= −0.58).

Subsequently, three additional patients from two families (subjects B1, C1 and C2) were identified. Subject B1 is a nondysmorphic, 11-year-old, African-American male born full term via cesarean section due to fetal distress after an otherwise uncomplicated pregnancy (Figure 1B). He exhibited his first seizure within the first 24 hours of life and was later diagnosed with medically intractable epilepsy. He is currently on multiple antiepileptics and has at least 3 distinct seizure types with approximately 3 breakthrough seizures per year. Subject B1 has normal growth parameters (FOC 55 cm, z=0.67, weight 45.2 kg, z=0.80, length 141 cm, z=−0.74).

Subjects C1 and C2 (previously described [16]) are children born to healthy, non-consanguineous south Indian parents (Figure 1C). Subject C1 is a 9-year-old female born at 33 weeks gestation with pregnancy complicated by premature rupture of membranes. She has medically intractable seizures that started on the 3rd day of life. She has been on numerous combinations of antiepileptics with at least 3 distinct seizure types and approximately 1–2 breakthrough seizure per month. Subject C1 has normal growth parameters (weight 26.8 kg, z = −0.85; length 125.2 cm, z = −1.7; FOC 50 cm, z = −0.96).

Subject C2 is an 8-year-old male born at 36 weeks gestation with pregnancy induced for fetal distress. His seizures started within the first 24 hours of life and despite medical management his seizures remain poorly controlled. He has at least 2 seizure types and his current seizure burden is approximately 1–2 seizures per month. Subject C2 has short stature (weight 23.7 kg, z = −0.82; length 118.4 cm, z = −2.04; FOC 51.5 cm, z = −0.42).

RESULTS

Sequencing Identifies Compound Heterozygous/Homozygous Mutations in *SLC13A5*

Whole exome sequencing (WES) of A1 and A2 identified 2 nonsynonymous, heterozygous variants in *trans* in *SLC13A5* that were not shared by the unaffected siblings. These missense variants (hg19; chr17: 6590948A>G, p.Leu492Pro; chr17: 6606350C>T, p.Gly219Arg) affected highly conserved residues with only the latter mutation previously observed in the NHLBI Exome Sequencing Project dataset and ExAC database with MAF of 0.014% and 0.035%, in European populations, respectively. Subject B1 harbors rare, compound heterozygous coding variants in *trans* configuration in *SLC13A5* (chr17:6599103G>A, p.Arg333X, MAF 0%; chr17:6606325G>A, p.Tyr227Met, MAF 0.0009%) (see Figure 1). Clinical WES of subjects C1 and C2 identified a homozygous *SLC13A5* mutation c.511delG (p.E1715fsX16) (see Figure 1), resulting in a frame shift and premature stop codon [16]. Parental Sanger sequencing studies confirmed each parent is heterozygous for this mutation.

Metabolomic profiling reveals altered TCA cycle intermediates

We conducted global metabolomic profiling by mass spectrometric analyses of urine (Subjects A1, A2, B1, and C1), plasma (subjects A1, A2, B1, C1, and C2), and CSF (subjects A1, A2, and B1) and compared the relative values of metabolites to unaffected control samples (N=80, 78, 76 for urine, plasma and CSF, respectively)[25,26]. In total, we identified 893, 629, 425 metabolites in the urine, plasma and CSF respectively (see Supplementary Table 1), of which, after removing unknown analytes and those involved in drug metabolism, 3, 4, and 25 were consistently and significantly perturbed when compared to controls (see Table 1 and Figure 2). We observed in both the CSF (p=1.3E-06) and the plasma (p=2.4E-04) an increase in the concentration of citrate when compared to controls (Figure 2A and B) but no significant difference in urine (p=0.34). A separate sample was clinically analyzed at a laboratory (ARUP labs, Salt Lake City Utah) for plasma citrate and demonstrated increased levels of citrate: 236, 120, and 118 umol/L for subjects A1, A2, and B1 respectively (reference range = 0–100 umol/L). These data were provided in Table 1B. These results are categorically identical to the MS results, but linear correlation is poor

owing in part to the small sample size and the samples were not taken on the same day (see Table 1B). Other TCA cycle intermediaries were also noted to be perturbed in the urine (fumarate) and CSF (isocitrate, 2-methylcitrate & aconitate).

Analysis of patients' CSF samples revealed consistent alterations in numerous metabolites compared to controls, including multiple metabolites associated with carbohydrate metabolism, lipid synthesis and amino acid pathways (Table 1). The most statistically significant metabolite in the CSF was beta-hydroxyisovaleroylcarnitine, an intermediate of leucine metabolism. Indeed, 6 of the 25 altered analytes in the CSF were involved directly with amino acid metabolism. The most over-abundant metabolite was 2-methylcitrate having an approximate 4-fold increase in relative amount in patient sample when compared to controls. In contrast, 3-hydroxybutyrate (BHBA) was the most under abundant metabolite. BHBA treatment has been used successfully to treat multiple acyl coenzyme A dehydrogenase deficiency [27]. In urine, fumarate was reduced in the subject samples compared to controls, demonstrating that disturbances of TCA cycle metabolites were detected in all three compartments (Table 1).

DISCUSSION

In this study, five subjects from three families with Early Infantile Epileptic Encephalopathy (EIEE25), global developmental delay, intellectual disability, and psychomotor retardation with biallelic mutations in *SLC13A5* are reported. *SLC13A5* expresses a sodium-coupled citrate transporter and has been shown in mouse liver to alter ATP/ADP ratios and modulate mitochondrial metabolism [14]. Citrate also acts as a source of energy, bicarbonate, potential chelator and as a biosynthetic precursor in the brain [28]. Interestingly, neurological phenotypes in mouse knockout models have not been reported nor do the subjects presented to date in the literature or here uniformly show decreased size or especially lean body-type as seen in the mouse knockout models. These differences in currently reported phenotypes may be due to, as yet, unrecognized differences in the function of SLC13A5 in humans and mice or differential redundancy effects of other tricarboxylic transporters between human and mouse brain. Affinity for citrate *in vitro* [10] is significantly different between the two homologs, which may have functional implications *in vivo*. Metabolic profiling of plasma in affected individuals showed multiple dysregulated analytes. Unlike the mouse model, we saw no significant reduction in plasma glucose or lactate levels. We did observe a significant increase in plasma citrate providing a metabolic signature that could be a useful diagnostic indicator of SLC13A5 dysfunction (Figure 2).

Metabolic analysis of CSF, plasma and urine revealed 32 dysregulated analytes in patients compared to controls (Figure 2, Table 1). The majority of perturbed analytes (25) were detected in the CSF, and the majority of the elevated analytes are involved with amino acid and energy metabolism. The only consistent dysregulated metabolite between plasma and CSF was citrate, consistent with the role of SLC13A5 in the liver. The range of metabolites dysregulated in the CSF may be an indication of general TCA dysregulation and indicative of the importance of the TCA in multiple metabolic and catabolic pathways (lipids, carbohydrates, amino acids and nucleotides). Given the important metabolic interrelationship between astrocytes and neurons, including the potential for astrocytes to

modulate neuronal excitability (Bélanger *et al.*, 2011), astrocyte dysfunction in SLC13A5 deficiency may be a key component of the pathophysiologic mechanism underlying the epileptic phenotype, but this hypothesis remains to be explored with future studies.

The two most dysregulated metabolites (i.e., the highest relative increase in patient CSF compared to control) were 2-methylcitrate and N6-succinyladenosine. N6-succinyladenosine accumulates in CSF, blood, and urine of patients with adenylosuccinate lyase (ADSL) deficiency [29]. Unlike ADSL deficiency, however, N6-succinyladenosine levels in SLC13A5 patients in urine (0.07), as well as in plasma ($p>0.42$), were indistinguishable from controls (−0.02, $p>0.78$). Further, there is no significant accumulation of SAICAR in any compartment tested. Patients with ADSL deficiency have neurological abnormalities, including seizures, and accumulation of N6-succinyladenosine and/or perturbation of the purine nucleotide cycle in the brain have been hypothesized to contribute to disease pathogenesis [30]. The elevation of N6-succinyladenosine in the CSF of SLC13A5 patients may reflect a secondary inhibition of ADSL in the brain. Whether accumulation of N6-succinyladensoine contributes to the pathogenesis of SLC13A5 deficiency remains an open question. Elevation of 2-methylcitrate is typically observed clinically in concert with elevations of methylmalonic acid and/or propionic acid as is seen in methylmalonic and propionic acidemias. 2-methylcitrate has been observed to inhibit glutamate oxidation and disturb mitochondrial energy homeostasis *in vitro* and, therefore, its accumulation in brain may also contribute to neuronal dysfunction in patients [31]. Interestingly, malonate is also elevated in the CSF of SLC13A5 patients (Table 1). Malonate is a competitive inhibitor of succinate dehydrogenase, which may further exacerbate the dysregulation of the TCA cycle, as well as potentially exacerbate neuronal excitotoxicity [32]. Given that astrocytes play an important role in metabolic compartmentation in the brain and through anaplerosis provide substrates for neuronal energy metabolism and neurotransmission [22], the significant alterations of multiple components of the TCA cycle in CSF suggest that, in addition to neuronal dysfunction, SLC13A5 deficiency may disrupt astrocyte energy metabolism and perturb metabolic compartmentation in the brain.

Metabolomic profiling of SLC13A5-deficient patients has allowed the generation of hypotheses regarding metabolic defects that may be present in astrocytes and neurons, but interpretation of the results is necessarily constrained due to lack of direct analysis of intracellular metabolism. Understanding and elucidating the underlying cellular defects and pathophysiology in the brain in the context of SLC13A5 deficiency is essential for the exploration of potential therapeutic approaches. Future studies using cell and animal models will be a critical component of that process.

Diagnosing an SLC13A5-related disorder early is critical for focusing treatment, prognosis and limiting unnecessary and redundant diagnostic tests. To date there are only anecdotal data suggesting that GABA modifying drugs, sodium channel inhibitors and acetazolamide may have efficacy in the treatment of seizures in SLC13A5 deficiency and further studies are needed to clarify the safety, efficacy and tolerability of the ketogenic diet [16,33]. Although genome wide sequencing can provide a definitive diagnosis in these cases, clinical sequencing is both expensive, has a relatively long turnaround time, poor rates of third-party reimbursement and may miss variants outside of the coding region. Clinically available

plasma organic acid testing provides a direct method for detecting increased plasma citrate levels but does not detect most TCA components. Mass-spectrometry based methods of interrogating the metabolome can provide a less expensive and more expeditious "hypothesis free" method to investigate potential diagnoses in an analogous way to genome wide sequencing [23,25]. High-throughput, metabolic profiling is a newly emerged and important tool for helping to establish a diagnosis for unknown metabolic diseases. It may be used alone, or in conjunction with DNA sequencing. Mass-spectrometric analysis has several advantages over DNA sequencing: It has a faster turn-around-time, is less expensive, and produces 2 orders of magnitude less data than whole exome sequencing, making interpretation less onerous. Whole exome sequencing, on the other hand, is more thorough for genetic disease and can diagnose non-metabolic disorders. However, metabolomics can also be useful in helping to establish pathogenicity of variants of unknown clinical significance or, in a research setting, help identify candidate genes and pathways for further analysis

Supplementary Material

Refer to Web version on PubMed Central for supplementary material.

Acknowledgments

The authors wish to thank the patients and their families for participating in this study.

Funding sources

This work was supported, in part, by the TESS Research Foundation (BHG); NIH/NIGMS R01 GM098387 (BHG).

References

1. McTague A, Howell KB, Cross JH, Kurian MA, Scheffer IE. The genetic landscape of the epileptic encephalopathies of infancy and childhood. Lancet Neurol. 152016; :304–316. DOI: 10.1016/S1474-4422(15)00250-1 [PubMed: 26597089]
2. Dulac O. Epileptic Encephalopathy. Epilepsia. 422001; :23–26. DOI: 10.1046/j.1528-1157.2001.042suppl.3023.x [PubMed: 11520318]
3. Fujiwara T, Sugawara T, Mazaki-Miyazaki E, Takahashi Y, Fukushima K, Watanabe M, Hara K, Morikawa T, Yagi K, Yamakawa K, Inoue Y. Mutations of sodium channel alpha subunit type 1 (SCN1A) in intractable childhood epilepsies with frequent generalized tonic-clonic seizures. Brain J Neurol. 1262003; :531–546.
4. Feucht M, Fuchs K, Pichlbauer E, Hornik K, Scharfetter J, Goessler R, Füreder T, Cvetkovic N, Sieghart W, Kasper S, Aschauer H. Possible association between childhood absence epilepsy and the gene encoding GABRB3. Biol Psychiatry. 461999; :997–1002. DOI: 10.1016/S0006-3223(99)00039-6 [PubMed: 10509183]
5. Cassandrini D, Cilio MR, Bianchi M, Doimo M, Balestri M, Tessa A, Rizza T, Sartori G, Meschini MC, Nesti C, Tozzi G, Petruzzella V, Piemonte F, Bisceglia L, Bruno C, Dionisi-Vici C, D'Amico A, Fattori F, Carrozzo R, Salviati L, Santorelli FM, Bertini E. Pontocerebellar hypoplasia type 6 caused by mutations in RARS2: definition of the clinical spectrum and molecular findings in five patients. J Inherit Metab Dis. 362013; :43–53. DOI: 10.1007/s10545-012-9487-9 [PubMed: 22569581]
6. Tavyev Asher YJ, Scaglia F. Molecular bases and clinical spectrum of early infantile epileptic encephalopathies. Eur J Med Genet. 552012; :299–306. DOI: 10.1016/j.ejmg.2012.04.002 [PubMed: 22548976]

7. Thevenon J, Milh M, Feillet F, St-Onge J, Duffourd Y, Jugé C, Roubertie A, Héron D, Mignot C, Raffo E, Isidor B, Wahlen S, Sanlaville D, Villeneuve N, Darmency-Stamboul V, Toutain A, Lefebvre M, Chouchane M, Huet F, Lafon A, de Saint Martin A, Lesca G, El Chehadeh S, Thauvin-Robinet C, Masurel-Paulet A, Odent S, Villard L, Philippe C, Faivre L, Rivière J-B. Mutations in SLC13A5 Cause Autosomal-Recessive Epileptic Encephalopathy with Seizure Onset in the First Days of Life. Am J Hum Genet. 952014; :113–120. DOI: 10.1016/j.ajhg.2014.06.006 [PubMed: 24995870]
8. Hardies K, de Kovel CGF, Weckhuysen S, Asselbergh B, Geuens T, Deconinck T, Azmi A, May P, Brilstra E, Becker F, Barisic N, Craiu D, Braun KPJ, Lal D, Thiele H, Schubert J, Weber Y, van 't Slot R, Nürnberg P, Balling R, Timmerman V, Lerche H, Maudsley S, Helbig I, Suls A, Koeleman BPC, Jonghe PD. Recessive mutations in SLC13A5 result in a loss of citrate transport and cause neonatal epilepsy, developmental delay and teeth hypoplasia. Brain. 2015; :awv263.doi: 10.1093/brain/awv263
9. Schossig A, Bloch-Zupan A, Lussi A, Wolf NI, Raskin S, Cohen M, Giuliano F, Jurgens J, Krabichler B, Koolen DA, de Macena Sobreira NL, Maurer E, Muller-Bolla M, Penzien J, Zschocke J, Kapferer-Seebacher I. SLC13A5 is the second gene associated with Kohlschütter-Tönz syndrome. J Med Genet. 542017; :54–62. DOI: 10.1136/jmedgenet-2016-103988 [PubMed: 27600704]
10. Inoue K, Zhuang L, Maddox DM, Smith SB, Ganapathy V. Structure, Function and Expression Pattern of a Novel Sodium-coupled Citrate Transporter (NaCT) Cloned from Mammalian Brain. J Biol Chem. 2772002; :39469–39476. DOI: 10.1074/jbc.M207072200 [PubMed: 12177002]
11. Gopal E, Miyauchi S, Martin PM, Ananth S, Srinivas SR, Smith SB, Prasad PD, Ganapathy V. Expression and functional features of NaCT, a sodium-coupled citrate transporter, in human and rat livers and cell lines. Am J Physiol - Gastrointest Liver Physiol. 2922007; :G402–G408. DOI: 10.1152/ajpgi.00371.2006 [PubMed: 16973915]
12. Rogina B, Reenan RA, Nilsen SP, Helfand SL. Extended Life-Span Conferred by Cotransporter Gene Mutations in Drosophila. Science. 2902000; :2137–2140. DOI: 10.1126/science.290.5499.2137 [PubMed: 11118146]
13. Toivonen JM, Walker GA, Martinez-Diaz P, Bjedov I, Driege Y, Jacobs HT, Gems D, Partridge L. No Influence of Indy on Lifespan in Drosophila after Correction for Genetic and Cytoplasmic Background Effects. PLoS Genet. 32007; :e95.doi: 10.1371/journal.pgen.0030095 [PubMed: 17571923]
14. Birkenfeld AL, Lee H-Y, Guebre-Egziabher F, Alves TC, Jurczak MJ, Jornayvaz FR, Zhang D, Hsiao JJ, Martin-Montalvo A, Fischer-Rosinsky A, Spranger J, Pfeiffer AF, Jordan J, Fromm MF, König J, Lieske S, Carmean CM, Frederick DW, Weismann D, Knauf F, Irusta PM, De Cabo R, Helfand SL, Samuel VT, Shulman GI. Deletion of the Mammalian INDY Homolog Mimics Aspects of Dietary Restriction and Protects against Adiposity and Insulin Resistance in Mice. Cell Metab. 142011; :184–195. DOI: 10.1016/j.cmet.2011.06.009 [PubMed: 21803289]
15. Schwarz F, Karadeniz Z, Fischer-Rosinsky A, Willmes DM, Spranger J, Birkenfeld AL. Knockdown of Indy/CeNac2 extends Caenorhabditis elegans life span by inducing AMPK/aak-2. Aging. 72015; :553–562. [PubMed: 26318988]
16. Klotz J, Porter BE, Colas C, Schlessinger A, Pajor AM. Mutations in the Na(+)/citrate cotransporter NaCT (SLC13A5) in pediatric patients with epilepsy and developmental delay. Mol Med Camb Mass. 222016; doi: 10.2119/molmed.2016.00077
17. Hadera MG, Smeland OB, McDonald TS, Tan KN, Sonnewald U, Borges K. Triheptanoin partially restores levels of tricarboxylic acid cycle intermediates in the mouse pilocarpine model of epilepsy. J Neurochem. 1292014; :107–119. DOI: 10.1111/jnc.12610 [PubMed: 24236946]
18. Shank RP, Bennett GS, Freytag SO, Campbell GL. Pyruvate carboxylase: an astrocyte-specific enzyme implicated in the replenishment of amino acid neurotransmitter pools. Brain Res. 3291985; :364–367. DOI: 10.1016/0006-8993(85)90552-9 [PubMed: 3884090]
19. Bergeron MJ, Clémençon B, Hediger MA, Markovich D. SLC13 family of Na+-coupled di- and tri-carboxylate/sulfate transporters. Mol Aspects Med. 342013; :299–312. DOI: 10.1016/j.mam.2012.12.001 [PubMed: 23506872]
20. Zhang Y, Chen K, Sloan SA, Bennett ML, Scholze AR, O'Keeffe S, Phatnani HP, Guarnieri P, Caneda C, Ruderisch N, Deng S, Liddelow SA, Zhang C, Daneman R, Maniatis T, Barres BA, Wu JQ. An RNA-sequencing transcriptome and splicing database of glia, neurons, and vascular cells

of the cerebral cortex. J Neurosci Off J Soc Neurosci. 342014; :11929–11947. DOI: 10.1523/JNEUROSCI.1860-14.2014

21. Zhang Y, Sloan SA, Clarke LE, Caneda C, Plaza CA, Blumenthal PD, Vogel H, Steinberg GK, Edwards MSB, Li G, Duncan JA, Cheshier SH, Shuer LM, Chang EF, Grant GA, Gephart MGH, Barres BA. Purification and Characterization of Progenitor and Mature Human Astrocytes Reveals Transcriptional and Functional Differences with Mouse. Neuron. 892016; :37–53. DOI: 10.1016/j.neuron.2015.11.013 [PubMed: 26687838]
22. Bélanger M, Allaman I, Magistretti PJ. Brain energy metabolism: focus on astrocyte-neuron metabolic cooperation. Cell Metab. 142011; :724–738. DOI: 10.1016/j.cmet.2011.08.016 [PubMed: 22152301]
23. Miller MJ, Kennedy AD, Eckhart AD, Burrage LC, Wulff JE, Miller LAD, Milburn MV, Ryals JA, Beaudet AL, Sun Q, Sutton VR, Elsea SH. Untargeted metabolomic analysis for the clinical screening of inborn errors of metabolism. J Inherit Metab Dis. 382015; :1029–1039. DOI: 10.1007/s10545-015-9843-7 [PubMed: 25875217]
24. Bainbridge MN, Hu H, Muzny DM, Musante L, Lupski JR, Graham BH, Chen W, Gripp KW, Jenny K, Wienker TF, Yang Y, Sutton VR, Gibbs RA, Ropers HH. De novo truncating mutations in ASXL3 are associated with a novel clinical phenotype with similarities to Bohring-Opitz syndrome. Genome Med. 52013; :11.doi: 10.1186/gm415 [PubMed: 23383720]
25. Kennedy AD, Miller MJ, Beebe K, Wulff JE, Evans AM, Miller LAD, Sutton VR, Sun Q, Elsea SH. Metabolomic Profiling of Human Urine as a Screen for Multiple Inborn Errors of Metabolism. Genet Test Mol Biomark. 202016; :485–495. DOI: 10.1089/gtmb.2015.0291
26. Kennedy AD, Pappan KL, Donti TR, Evans AM, Wulff JE, Miller LAD, Sutton VR, Sun Q, Miller MJ, Elsea SH. Elucidation of the complex metabolic profile of cerebrospinal fluid using an untargeted biochemical profiling assay. Mol Genet Metab. 1212017; :83–90. DOI: 10.1016/j.ymgme.2017.04.005 [PubMed: 28412083]
27. Van Rijt WJ, Heiner-Fokkema MR, du Marchie Sarvaas GJ, Waterham HR, Blokpoel RGT, van Spronsen FJ, Derks TGJ. Favorable outcome after physiologic dose of sodium-D,L-3-hydroxybutyrate in severe MADD. Pediatrics. 1342014; :e1224–1228. DOI: 10.1542/peds.2013-4254 [PubMed: 25246622]
28. Pajor AM. Sodium-coupled dicarboxylate and citrate transporters from the SLC13 family. Pflüg Arch - Eur J Physiol. 4662013; :119–130. DOI: 10.1007/s00424-013-1369-y
29. Donti TR, Cappuccio G, Hubert L, Neira J, Atwal PS, Miller MJ, Cardon AL, Sutton VR, Porter BE, Baumer FM, Wangler MF, Sun Q, Emrick LT, Elsea SH. Diagnosis of adenylosuccinate lyase deficiency by metabolomic profiling in plasma reveals a phenotypic spectrum. Mol Genet Metab Rep. 82016; :61–66. DOI: 10.1016/j.ymgmr.2016.07.007 [PubMed: 27504266]
30. Jurecka A, Zikanova M, Kmoch S, Tylki-Szymańska A. Adenylosuccinate lyase deficiency. J Inherit Metab Dis. 382015; :231–242. DOI: 10.1007/s10545-014-9755-y [PubMed: 25112391]
31. Amaral AU, Cecatto C, Castilho RF, Wajner M. 2-Methylcitric acid impairs glutamate metabolism and induces permeability transition in brain mitochondria. J Neurochem. 1372016; :62–75. DOI: 10.1111/jnc.13544 [PubMed: 26800654]
32. Greene JG, Greenamyre JT. Exacerbation of NMDA, AMPA, and L-glutamate excitotoxicity by the succinate dehydrogenase inhibitor malonate. J Neurochem. 641995; :2332–2338. [PubMed: 7536810]
33. Hardies K, de Kovel CGF, Weckhuysen S, Asselbergh B, Geuens T, Deconinck T, Azmi A, May P, Brilstra E, Becker F, Barisic N, Craiu D, Braun KPJ, Lal D, Thiele H, Schubert J, Weber Y, van 't Slot R, Nürnberg P, Balling R, Timmerman V, Lerche H, Maudsley S, Helbig I, Suls A, Koeleman BPC, De Jonghe P. autosomal recessive working group of the EuroEPINOMICS RES Consortium. Recessive mutations in SLC13A5 result in a loss of citrate transport and cause neonatal epilepsy, developmental delay and teeth hypoplasia. Brain J Neurol. 1382015; :3238–3250. DOI: 10.1093/brain/awv263

Highlights

- SCL13A5 deficientcy shows disrupted citrate in plasma that is readily detectable by mass-spectrometry
- Multiple metabolites of the citrtic acid cycle and downstream analytes, including neurotransmitters, are disrupted in the CSF
- Mass-spectrometry of CSF can be used to identify SLC13A5 deficiency and inform whole exome sequencing results

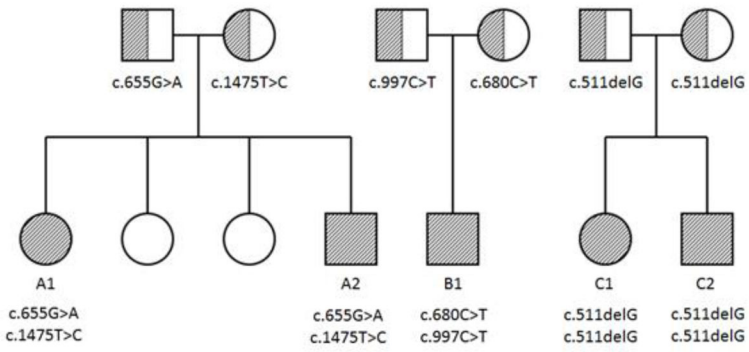

Figure 1.

Pedigree, disease and mutation status for three families, A, B and C. Hashing indicates disease/carrier status (full/half, respectively).

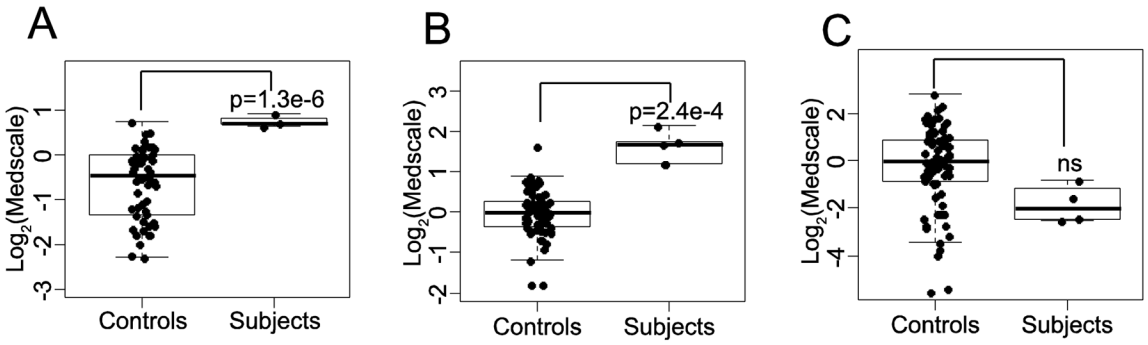

Figure 2. Citrate is elevated in plasma and CSF in *SLC13A5* patients

Box and whisker plots of (A) CSF (n=3) (B) plasma (n=5) and (C) urine (n=4) citrate levels between controls and subjects.

Table 1

Analytes with significant perturbations between in SLC13A5 deficient subjects and controls

Analyte name, median centered, log-transformed values for each subject, as well as mean value for subjects and controls is shown with p-value and false discovery rate for (A) CSF, (B) plasma, and (C) urine. Unknown analytes and drug metabolism analytes excluded. Under Fold Diff column, green indicates relative elevation in patients while blue indicates relative decrease.

A. CSF								
COMPOUND	**Pathway**	**A1**	**A2**	**B1**	**Subject Avg**	**Control Avg**	**Fold Diff**	**FDR**
beta-hydroxyisovaleroylcarnitine	Amino Acid	0.80	0.73	0.76	0.76	−0.03	1.73	5.81E-17
S-1-pyrroline-5-carboxylate		1.87	1.47	1.61	1.65	0.71	1.92	6.74E-03
acisoga		−1.50	−1.09	−1.50	−1.36	−0.03	0.40	9.25E-03
cystathionine		−0.14	−0.14	0.22	−0.02	−0.93	1.88	9.25E-03
N-acetylasparagine		0.58	0.31	0.38	0.43	−0.18	1.53	4.04E-02
imidazole propionate		−0.01	0.00	−0.01	−0.01	0.66	0.63	4.18E-02
erythronate	Carbohydrate	0.65	0.41	0.55	0.53	−0.10	1.55	4.18E-02
isocitrate	Energy	1.22	1.21	1.21	1.21	0.22	1.99	3.56E-07
2-methylcitrate		1.28	1.01	1.15	1.15	−0.66	3.51	4.11E-07
citrate		0.64	0.71	0.92	0.76	−0.84	3.03	2.42E-05
aconitate		−0.20	−0.14	0.13	−0.07	−1.23	2.23	3.03E-04
malonate	Lipid	0.41	0.52	0.46	0.46	−1.01	2.77	5.81E-17
3-hydroxybutyrate (BHBA)		−2.51	−2.79	−2.94	−2.75	−0.68	0.24	9.28E-07
1-arachidonoyl-GPE		−1.19	−1.19	−1.19	−1.19	−0.28	0.53	9.64E-06
1,2-dioleoyl-GPC		0.83	0.56	0.75	0.71	−0.15	1.82	4.90E-04
3-hydroxyoctanoate		−0.95	−0.96	−0.85	−0.92	−0.35	0.67	1.16E-03
phosphocholine		−0.54	−0.45	−0.64	−0.54	−0.03	0.70	1.33E-03
1-stearoyl-2-linoleoyl-GPC		0.48	0.14	0.52	0.38	−0.66	2.06	6.22E-03
3-aminoisobutyrate	Nucleotide	−1.61	−1.62	−1.27	−1.50	−0.36	0.45	1.16E-03
N6-succinyladenosine		1.65	1.11	1.48	1.41	−0.23	3.12	4.96E-03
succinimide	Xenobiotics	−1.72	−1.71	−1.73	−1.72	−0.24	0.36	3.94E-13
trizma acetate		0.61	0.62	0.76	0.66	−0.42	2.11	1.04E-03
tartarate		0.69	0.91	0.73	0.78	0.12	1.58	1.16E-03

A. CSF								
COMPOUND	**Pathway**	**A1**	**A2**	**B1**	**Subject Avg**	**Control Avg**	**Fold Diff**	**FDR**
7-methylxanthine		−0.01	−0.01	0.00	−0.01	0.72	0.60	1.79E-02
S-allylcysteine		−0.01	−0.01	−0.01	−0.01	0.77	0.58	3.91E-02

B. Plasma										
COMPOUND	**Pathway**	**A1**	**A2**	**B1**	**C1**	**C2**	**Subject Avg**	**Control Avg**	**Fold Diff**	**FDR**
pyroglutamine	Amino Acid	1.84	1.93	1.67	1.01	2.06	1.7	0.24	0.53	0.006
N-6-trimethyllysine		−0.35	−0.04	−0.23	−0.34	−0.21	−0.23	0.15	0.76	0.03
eicosanodioate	Lipid	−1.32	−0.76	−1.21	−0.34	−1.22	−1.34	−0.26	0.53	0.003
citrate	TCA Cycle	1.69	1.21	2.14	1.21	1.74	1.6	−0.04	3.10	0.02

C. Urine									
COMPOUND	**Pathway**	**A1**	**A2**	**B1**	**C1**	**Subject Avg**	**Control Avg**	**Fold Diff**	**FDR**
16a-hydroxy DHEA 3-sulfate	Steroid	4.46	N/D	3.99	3.82	4.09	0.75	10.16	2.E-05
lactate	Pyruvate	−1.89	−1.06	−1.90	−1.11	−1.49	0.27	0.29	0.04
fumarate	TCA Cycle	−1.68	−1.69	−2.83	−1.57	−1.94	0.13	0.23	0.05

N/D: Not detected